



HAL
open science

Understanding *Chlorella vulgaris* acclimation strategies on textile supports can improve the operation of biofilm-based systems

Su Fang Li, Andrea Fanesi, Thierry Martin, Filipa Lopes

► **To cite this version:**

Su Fang Li, Andrea Fanesi, Thierry Martin, Filipa Lopes. Understanding *Chlorella vulgaris* acclimation strategies on textile supports can improve the operation of biofilm-based systems. *Journal of Applied Phycology*, 2023, 35 (3), pp.1061-1071. 10.1007/s10811-023-02963-8. hal-04427813

HAL Id: hal-04427813

<https://hal.science/hal-04427813>

Submitted on 31 Jan 2024

HAL is a multi-disciplinary open access archive for the deposit and dissemination of scientific research documents, whether they are published or not. The documents may come from teaching and research institutions in France or abroad, or from public or private research centers.

L'archive ouverte pluridisciplinaire **HAL**, est destinée au dépôt et à la diffusion de documents scientifiques de niveau recherche, publiés ou non, émanant des établissements d'enseignement et de recherche français ou étrangers, des laboratoires publics ou privés.

1 **Understanding *Chlorella vulgaris* acclimation strategies on textile supports can**
2 **improve the operation of biofilm-based systems**

3

4 **Su Fang Li, Andrea Fanesi, Thierry Martin, Filipa Lopes***

5 *Laboratoire Génie des Procédés et Matériaux (LGPM), CentraleSupélec, Université Paris-*
6 *Saclay, 91190 Gif-sur-Yvette, France*

7 ** Corresponding author*

8 *E-mail address: filipa.lopes@centralesupelec.fr*

9

10 **Abstract**

11 The interest in microalgae biofilm-based systems has been increasing lately due to their high
12 potential for biomass production. However, more studies focusing on the first stages of this
13 bioprocess, such as support selection and inoculum properties, which may finally affect biomass
14 productivity, are required. The aim of this study was therefore to assess the impact of support
15 nature and inoculum properties on microalgae biofilm productivity and physiology. Results
16 suggest that physico-chemical properties of the support (micro-texture, hydrophobicity and
17 chemical functional groups) affect the attachment of *Chlorella vulgaris*. Significant differences in
18 cell-distribution pattern and biofilm structure on polyamide-based (Terrazzo) and cotton-based
19 fabrics were observed. Compared to Cotton, cells grown on Terrazzo showed higher biomass
20 productivity (3.20-fold), photosynthetic capacity (1.32-fold) and carbohydrate pool (1.36-fold),
21 which may be explained by differences in light availability due to support micro-texture. A high
22 inoculum density resulted in a lower biofilm growth, likely due to a lower light/nutrient
23 availability for the cells. Furthermore, when immobilized on fabrics, cells pre-acclimated to 350

1 $\mu\text{mol photons m}^{-2} \text{ s}^{-1}$ grew faster than those pre-acclimated to low light ($50 \mu\text{mol photons m}^{-2} \text{ s}^{-1}$),
2 demonstrating the influence of light-history of the inoculum cells on biofilm productivity.
3 Therefore, this work confirmed the importance of support and inoculum properties for biofilm-
4 based systems.

5
6 **Keywords**

7 *Chlorella vulgaris*, Microalgae biofilms, Physiological properties, Biofilm structure, Textile
8 materials

9
10 **Declarations**

11 **Funding**

12 S. F. Li was supported by the China Scholarship Council (CSC) and the authors would like to
13 thanks for founding the LabeX LaSIPS project Greenbelt and the ANR project
14 PhotobiofilmExplorer (ANR-20-CE43-0008) managed by the French National Research Agency
15 (ANR).

16 **Competing interests**

17 The authors declare no competing interests.

18 **Availability of data and material**

19 Not applicable

20 **Code availability**

21 Not applicable

22 **Authors' contributions**

23 S. F. Li, A. Fanesi, T. Martin and F. Lopes designed the experiments, S. F. Li and A. Fanesi

1 conducted the experiments, S. F. Li, A. Fanesi and F. Lopes analyzed the data, S. F. Li and A.
2 Fanesi wrote the manuscript, F. Lopes revised the article. All authors read and approved the final
3 manuscript.

4

5 **Acknowledgements**

6 The authors would like also to acknowledge Nathalie Ruscassier for SEM observation, Jamila El
7 Bekri for contact angle measurement and H  l  ne Santigny for her technical support during the
8 experiments.

1 **1. Introduction**

2 The interest in microalgae biofilm-based systems has been increasing lately due to their
3 advantages, such as lower costs of harvesting, energetic consumption and water demands
4 (Johnson and Wen 2010; Christenson and Sims 2012; Gross et al. 2015), with respect to
5 conventional suspended cultures where cells are in a planktonic state. Studies proposing
6 innovative designs and culture optimization have been thus carried out to fully confirm the
7 feasibility of the biofilm approach for large-scale cultivation (Genin et al. 2014; Li et al. 2017).

8 The inoculation step is of paramount importance on microalgae bioprocess development.
9 Indeed, it affects biomass productivity and yield (Genin et al. 2014; Moreno Osorio et al. 2020;
10 Li et al. 2021). Biofilm productivity can be clearly improved by increasing the inoculum size
11 (Zhang et al. 2014; Ji et al. 2014; Shen et al. 2017) but eventually light attenuation and/or
12 nutrients limitation may occur thereby decreasing biomass productivity (Huang et al. 2016; Li et
13 al. 2021). Support properties such as hydrophobicity, roughness and surface free energy influence
14 cells colonization efficiency by changing affinity and cell interactions with the substrate (Ozkan
15 and Berberoglu 2011; Cui et al. 2013; Gross et al. 2016; Huang et al. 2018; Tsavatopoulou and
16 Manariotis 2020). Interestingly, Vivier et al. (2021) demonstrated that the microtopography of
17 colonized substrates can also affect biofilm physiology. Rough supports seem to create local
18 microhabitats that may help protect cells from photo-inhibition.

19 Among supports for microalgae biofilm development, fabrics have been studied due to their
20 flexibility, easy microalgae re-growth after harvesting and low cost compared with other
21 materials (Gross et al. 2013; Gross and Wen 2014; Moreno Osorio et al. 2019; Hart et al. 2021).
22 The majority of these works reported macroscopic data such as biofilm overall productivity
23 (Gross and Wen 2014; De Assis et al. 2019; Brockhagen 2021) and only few described

1 microscale patterns (e.g. cell distribution on the support/biofilm structure) (Moreno Osorio et al.
2 2020) or assessed the interplay between fabrics properties and the physiological state of the cells.
3 Supports selection should be therefore carefully considered in biofilm process optimization.

4 In planktonic cultures, a broad number of studies show that cellular traits such as chlorophyll
5 content or cell size strongly affect growth dynamics of microalgae populations (Post et al. 1984;
6 Sukenik et al. 1990; Urabe and Kagami 2001; MacIntyre et al. 2002). For example, the lower the
7 chlorophyll quota, the more transparent the microalgae and the higher the growth rate or
8 productivity achieved (Sukenik et al. 1990; MacIntyre et al. 2002; Martínez et al. 2018). Some
9 others also reported a decrease in the algal growth rate with the increasing cell size (Urabe and
10 Kagami 2001; Key et al. 2010; López-Sandoval et al. 2014). From these observations, it is clear
11 that the light-history of microalgae may play an important role in biofilm processes, nevertheless
12 at present no information on the subject is available.

13 In this work, we aim at assessing the impact of fabric nature, inoculum density and its
14 physiology on *C. vulgaris* biofilm initial colonization, productivity and composition (3 days).
15 First, in order to select appropriate fabrics for biofilm development, cells attachment/detachment
16 on five textile materials were investigated. The interplay between surface properties (i.e., relative
17 opening surface area, hydrophobicity, chemical functional groups etc.) and cells retention
18 capability was afterwards discussed. Cotton, considered as an excellent material for biofilm
19 development (Christenson and Sims 2012; Gross et al. 2013), and a polyamide-based fabric with
20 the highest cells retention capability from our study, were then chosen to evaluate the impact of
21 support characteristics on biofilm production, activity and composition. The structure of biofilms
22 formed on the selected fabrics, seldom described in the literature, was characterized using
23 complementary imaging tools (CLSM - Confocal Laser Scanning Microscopy and SEM -

1 Scanning Electron Microscopy). Finally, in order to test our hypothesis that the physiological
2 status of the inoculum cells affects biofilm growth, cells photo-acclimated to low or high light
3 were immobilized and their growth, composition and photosynthetic activity were measured after
4 3 days of growth.

5

6 **2. Materials and Methods**

7 *2.1. Planktonic culture maintenance*

8 *Chlorella vulgaris* SAG 211–11b (Göttingen, Germany) was cultured semi-continuously in 1-
9 L bottles filled with 800 mL 3N-Bristol medium (Bischo and Bold 1963) at 25°C. The cultures
10 were bubbled with filtered air under a continuous illumination of 50 (low light, LL) and 350
11 $\mu\text{mol photons m}^{-2} \text{s}^{-1}$ (high light, HL) (Viugreum 50W LED, Biospherical Instruments, San
12 Diego, CA, USA; the irradiance was measured inside the cultures using a QSL-2100 quantum
13 scalar irradiance sensor). The cultures were kept in exponential phase with a maximum cell
14 concentration of 5.8×10^6 cells mL^{-1} by daily dilution in order to maintain a chlorophyll (Chl) *a*
15 concentration of 0.5 - 1.5 mg Chl *a* L^{-1} to ensure optimal light penetration. The planktonic
16 cultures were pre-acclimated to 50 or 350 $\mu\text{mol photons m}^{-2} \text{s}^{-1}$ for at least 8 days before starting
17 any experiments.

18

19 *2.2. Textile supports characterization*

20 Five textile materials (see table S1_supplementary data for more details) were purchased on
21 <https://www.tissusactifs.fr> and their micro-texture and physico-chemical properties were
22 characterized with several techniques.

1 The micro-texture of the materials was observed using a stereomicroscope (Zeiss, Discovery
2 V12, Germany). The images were taken in a size of 2.30 mm × 1.72 mm with 63× magnification
3 (Fig. S1_supplementary data). The area of the pores on the surface of each material was
4 quantified using the Fiji software (Kostajnsšek et al. 2021). The relative opening surface area (i.e.,
5 the total opening area in 1 cm² of textile) was afterwards calculated.

6 The surface roughness of the textile materials was quantified using a microtopographe (STIL
7 CHR 150, France). At least five positions on each material were randomly selected for roughness
8 determination. The surface roughness (Ra) was analyzed by the Mountains Map Universal
9 software (Digital Surf Sarl 3.0, Besancon, France).

10 The hydrophobicity of textile materials was determined using the sessile drop test with an
11 automatic drop tensiometer (Tracker Teclis/IT Concept, France). 5 μL of distilled water (as
12 reference liquid) was pipetted onto the surface of the materials, and the images of water drops
13 were analyzed using WDROP 2010 software to characterize the static water contact angle (θ)
14 which reflects surface hydrophobicity ($0^\circ < \theta \leq 90^\circ$, hydrophilic surface; $90^\circ < \theta < 180^\circ$,
15 hydrophobic surface; $\theta = 180^\circ$, ultra-hydrophobic surface, respectively) (Van Oss et al. 1988).

16 An ATR-FTIR (Fourier Transform Infrared Spectrometer with Attenuated Total Reflectance)
17 PerkinElmer Spectrum-two spectrometer (PerkinElmer, Waltham, MA, USA) was used to
18 analyze the chemical properties of the textile materials. Infrared spectra were recorded in the
19 range of 4000 to 400 cm⁻¹ using an accumulation of 32 scans at a spectral resolution of 4 cm⁻¹.
20 Before loading materials, the empty crystal was measured as background.

21

22

23 *2.3. Selection of textile supports for biofilm growth*

1 A first screening of supports was done based on the criteria of cells-retention capability (i.e.,
2 how many cells were retained on the support) after cell immobilization. The fabric with the
3 highest number of retained cells was then selected for further studies along with cotton (widely
4 described in the literature). Textiles were first cut into squares of 2.4×2.4 cm and sterilized in
5 Milli-Q water at 121°C for 15 min. Aliquots of 2 mL concentrated planktonic cultures (1.0×10^7
6 cells mL^{-1}) were afterwards filtered on the textile materials (with a colonization area of 2.01 cm^{-2}).
7 2).

8 After 6-h incubation in 6-well culture plates (Thermo Fisher Scientific, Inc.; each well filled
9 with 8 mL 3N-Bristol medium), the cells on textile materials were harvested by vigorously
10 vortexing the fabrics (for 5 min with 10 mL of growth medium) in 50 mL centrifugation tubes
11 (containing glass beads). Then, the cells in solution (detached fraction), and those on textile
12 materials (successfully immobilized fraction) were quantified using flow cytometry (Guava
13 EasyCyte HT; Millipore, USA).

14

15 *2.4. Immobilization and growth of C. vulgaris on textile supports*

16 Two initial cell densities corresponding to $(1.5 \pm 0.2) \times 10^6$ cells cm^{-2} (low inoculum cell
17 density, LC, $0.2 \pm 0.02 \text{ g m}^{-2}$) and $(7.0 \pm 1.4) \times 10^6$ cells cm^{-2} (high inoculum cell density, HC,
18 $0.8 \pm 0.16 \text{ g m}^{-2}$) were obtained by filtrating specific volumes of planktonic culture on Cotton and
19 Terrazzo. More precisely, after a 10-times filtration of the same algal solution, each textile
20 material was washed gently in Petri dishes to remove the loosely attached cells and placed in
21 multi-well culture plates under $100 \mu\text{mol photons m}^{-2} \text{ s}^{-1}$. One coupon was immediately used to
22 verify the cell number just after the inoculation step. Coupons were incubated for three days and
23 the medium was completely renewed every day to avoid nutrient limitation.

1

2 *2.5. Immobilized growth of C. vulgaris pre-acclimated to two light intensities*

3 In order to test the impact of light-history of the inoculum on biofilm growth, composition
4 and activity, cells pre-acclimated to 50 (LL-acclimated cells) and 350 $\mu\text{mol photons m}^{-2} \text{s}^{-1}$ (HL-
5 acclimated cells) were filtrated on Terrazzo with low initial cell density $(1.5 \pm 0.2) \times 10^6 \text{ cells cm}^{-2}$
6 and then exposed to 100 $\mu\text{mol photons m}^{-2} \text{s}^{-1}$. After 3 days, the cells that colonized the fibers
7 were harvested as described above and further measurements such as productivity,
8 photosynthesis and macromolecular composition were carried out (see below for details). Here,
9 biofilms formed from cells photo-acclimated to 50 $\mu\text{mol photons m}^{-2} \text{s}^{-1}$ were named as LL
10 biofilms (Biofilms Produced with Low Light acclimated cells) and those formed from cells
11 photo-acclimated to 350 $\mu\text{mol photons m}^{-2} \text{s}^{-1}$ as HL biofilms (Biofilms Produced with High
12 Light acclimated cells).

13

14 *2.6. Relative biomass increase and biomass productivity on textile supports*

15 Although several harvesting steps were performed, no full cell recovery was achieved.
16 Therefore, in order to fully estimate the immobilized biomass, Chl *a* from cells on the coupons
17 was extracted according to the method described in section 2.7b. The number of residual cells
18 was afterwards estimated based on the average cellular Chl *a* content of the mechanically
19 recovered cells.

20 The relative biomass increase to the initial population on coupon (R_c) was calculated as
21 following according to Eq. (1):

22
$$R_c = [(C_m + C_{chl}) - C_0]/C_0 \tag{1}$$

1 where C_m and C_{chl} represent cell numbers obtained by mechanically harvesting and by Chl *a*-
2 content measurements after 3 days, respectively, whereas C_0 stands for the cells on supports at
3 the beginning of the experiment.

4 Similarly, biomass productivity (P_x , $g\ m^{-2}\ d^{-1}$) was calculated according to Eq. (2):

$$5\quad Px = [(X_m + W_t * C_{chl}/S) - X_0]/t \quad (2)$$

6 where X_m and X_0 represent biomass areal density ($g\ m^{-2}$) obtained by mechanically harvesting
7 after 3 days and at the beginning of the experiment, respectively; whereas W_t stands for the
8 average cell dry weight ($g\ cell^{-1}$), which was estimated by the mechanically harvested biomass
9 after t (here $t = 3, d$) days; and S is the area (m^2) of the attached culture.

10

11 2.7. Physiological traits of sessile cells

12 Average cell diameter was determined considering a minimum of 300 individual cells using
13 an AxioSkop 2 plus microscope (Carl Zeiss, Oberkochen, Germany) and a 63× magnification
14 lens. Cell volume was calculated using the formula reported by Hillebrand et al. (1999).

15 Chl *a* was extracted using dimethyl sulfoxide (DMSO), and quantified by measuring the
16 absorption at 649 nm and 665 nm with an Evolution 60S UV–visible spectrophotometer (Thermo
17 Scientific, Madison, WI, USA). The Chl *a* concentration was calculated by the equation reported
18 by Wellburn (1994).

19 Photosynthetic activity of immobilized *C. vulgaris* was assessed using a Pulse Amplitude
20 Modulation (PAM) fluorometer (AquaPen, AP 110-C, Photon Systems Instruments, Drasov,
21 Czech Republic). After 10 min of dark-adaptation, the relative electron transport rates (rETR_s)
22 corresponding to seven increasing actinic lights were used to construct the rapid light curve

1 (RLC) as described in (Li et al. 2021). The maximum rETR ($rETR_{\max}$) was obtained from the
2 RLC fitting function (Webb et al. 1974):

$$3 \quad rETR = rETR_{\max} (1 - e^{-\alpha I / rETR_{\max}}) \quad (3)$$

4 where α represents the initial slope of RLC curve and photo-saturation E_k was computed from
5 $E_k = rETR_{\max} / \alpha$. Additionally, the maximum quantum yield F_v/F_m was calculated with the
6 equation:

$$7 \quad F_v/F_m = (F_m - F_0)/F_m \quad (4)$$

8 where F_0 and F_m are the minimum and max fluorescence determined after 10 min dark-
9 adaptation, respectively, and F_v indicates the variable fluorescence.

10 The macromolecular composition of the cells was characterized using ATR-FTIR-
11 spectroscopy (PerkinElmer, Waltham, MA, USA). The FTIR spectra of cells were baselined and
12 maximum absorption values in the spectral ranges corresponding to carbohydrates (C–O–C;
13 $1200\text{--}950\text{ cm}^{-1}$), lipids (C=O; $1750\text{--}1700\text{ cm}^{-1}$) and proteins (Amide I; $1700\text{--}1630\text{ cm}^{-1}$) were
14 used to calculate the relative carbohydrates and lipids contents to proteins (Fanesi et al. 2019; Li
15 et al. 2021).

16

17 *2.8. Textile biofilms imaging*

18 The overall cell distribution on Cotton and Terrazzo was assessed by stereomicroscopy.
19 Images were taken in a size of $1.72\text{ mm} \times 1.72\text{ mm}$ with $63 \times$ magnification. Biofilm structure
20 was assessed by CLSM using an inverted Zeiss LSM700 confocal microscope (Carl Zeiss
21 microscopy GmbH, Jena, Germany) equipped with a LD Plan-Neofluar $20\times/0.4$ Korr M27
22 objective with a 0.4 N.A. (numerical aperture) (Fanesi et al. 2019). Cells were detected by the

1 chlorophyll *a* autofluorescence at 639 nm. The images were $640 \times 640 \mu\text{m}$ in size with a z-step of
2 $3.94 \mu\text{m}$ and a lateral resolution of $1.25 \mu\text{m}$.

3 In order to further investigate the interaction of algal cells with the fabrics, a scanning
4 electron microscope (ESEM, FEI Quanta 200) was used to obtain SEM images with $2000\times$
5 magnification. A small piece of support ($5 \text{ mm} \times 5 \text{ mm}$) was examined at 20 kV accelerating
6 voltage with a working distance of 14 mm in a high vacuum mode. The chamber was precooled
7 to $7 \sim 8 \text{ }^\circ\text{C}$ and the determination of samples was carried out in a solid-liquid phase. Each support
8 observation was performed in at least three random positions.

9 In addition, biofilm formation on Terrazzo inoculated with a LC-inoculum (Low cell density,
10 $\sim 1.5 \times 10^6 \text{ cells cm}^{-2}$) was observed by Optical Coherence Tomography (OCT; Ganymede 621,
11 Thorlabs GmbH, luebeck, Germany). The field of view was $4 \times 4 \text{ mm}$ (XY) and the axial depth
12 was 1 mm (Z). The lateral and axial resolution were $8 \mu\text{m}$ and $1.45 \mu\text{m}$, respectively. A
13 refractive index of 1.33 was used for in-situ image acquisitions as the biofilm was aqua-cultured
14 (Wagner and Horn 2017; Fanesi et al. 2022). Images were then analysed using the software
15 ThorImageOCT 5.4.4 (Thorlabs, luebeck, Germany).

16

17 *2.9. Statistical analysis*

18 All results were presented as mean values \pm standard deviations ($n \geq 3$). After the tests of
19 normality (Shapiro-Wilk test) and variance homogeneity (Levene's test), one-way ANOVA
20 analysis of variance followed by Tukey's post hoc test for multiple comparisons in cells,
21 attachment/detachment and physico-chemical properties among different textiles were carried out
22 using IBM SPSS Statistics 25.0 (SPSS Inc., Chicago, IL). Significant differences in cells growth,

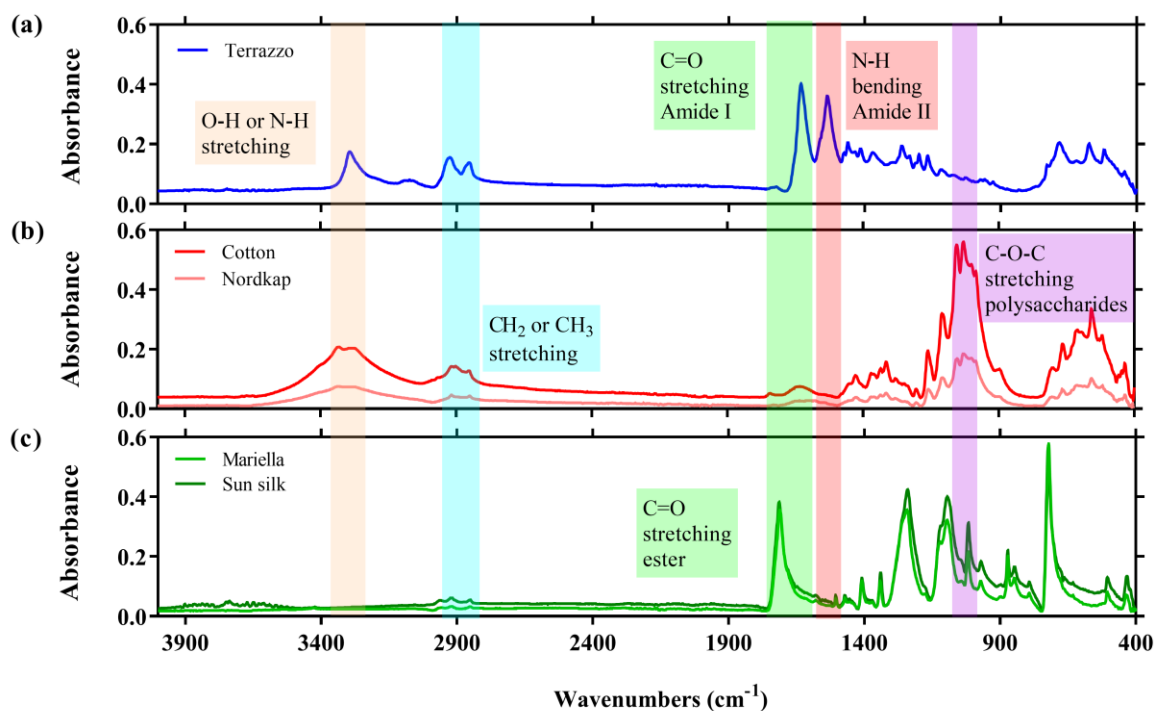
1 activity, composition and biofilm productivity between different treatments (two supports, two
2 inoculum densities and two inoculum pre-acclimated light intensities) were performed by
3 Students's *t*-tests with pairwise comparisons testing. The statistical significance of the data was
4 shown at the levels of $P < 0.05$, $P < 0.01$ or $P < 0.001$.

5

6 **3. Results**

7 *3.1. Support characterization and selection for C. vulgaris immobilized growth*

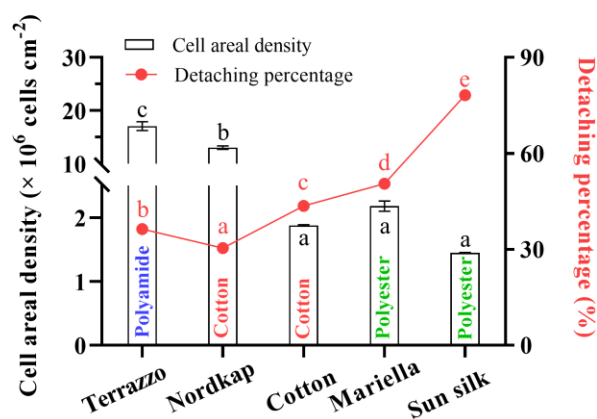
8 Characteristic peaks from 2900 to 3500 cm^{-1} were detected on the polyamide-based
9 (Terrazzo) and on the cotton-based supports (Cotton and Nordkap, Fig. 1) suggesting the
10 existence of O-H, N-H and C-H bonds (Shahzadi et al. 2018). Two peaks at 1633 and 1537 cm^{-1}
11 corresponding to C=O stretching in amide-I and N-H bending in amide-II, respectively, were
12 observed only on Terrazzo (Kang et al. 2012; Shahzadi et al. 2018). Also, a peak at 1038 cm^{-1}
13 related to the C-O bonds (Chung et al. 2004) in polysaccharides was found on cotton-based
14 substrata. In the polyester-based supports (Sun silk and Mariella), the C=O bond at 1712 cm^{-1}
15 indicated the presence of ester functional groups (Hoghoghifard et al. 2016).



1
 2 **Fig. 1** FTIR-spectra of five fabrics (a, polyamide-based textile; b, cotton-based textile; c,
 3 polyester-based textile. Main functional groups in the fabrics are highlighted by different colors)
 4 used as a growth support for microalgae biofilm cultivation

5
 6 Supports were further characterized in terms of hydrophobicity, roughness and relative pore
 7 surface opening size (Table S1_supplementary data). All supports but Sun silk and Mariella were
 8 hydrophobic (contact angle $\theta > 90^\circ$). In addition, similar roughness values (30 – 50 μm) were
 9 detected for all materials except Terrazzo which is smoother (*ca.* 16 μm). Moreover, a broad
 10 range of opening sizes, which are larger than *C. vulgaris* cells (2-10 μm), was quantified for each
 11 material except for Terrazzo for which no surface opening was detected (Fig. S1_supplementary
 12 data).

1 Fig. 2 shows cells retention and detachment for the different textiles after 6 hours from
 2 inoculation. High cell retention capability and low releasing percentages were found for Terrazzo
 3 (17.1×10^6 cells cm^{-2} , 36.3%) and Nordkap fabrics (13.1×10^6 cells cm^{-2} , 30.4%). However,
 4 similar low values of cell areal densities and high releasing percentages were obtained for Cotton
 5 and the polyester-based supports, Mariella and Sun silk ($\sim 1.8 \times 10^6$ cells cm^{-2} , 45 - 80%).
 6 Among cotton-based supports, Nordkap presented a higher cell retention capability compared to
 7 Cotton though similar physico-chemical properties (surface chemical functional groups,
 8 hydrophobicity, roughness) were determined for both supports (Fig. 2, Table S1_supplementary
 9 data). Finally, the highest cell areal density and low detachment were obtained for Terrazzo.
 10



11
 12 **Fig. 2** Cell areal density on different textile materials after 6-h incubation. All the results are
 13 shown as mean value \pm SD, $n = 3$; Bars and dots with different letters represent the statistical
 14 differences among different textiles at a level of $P < 0.05$

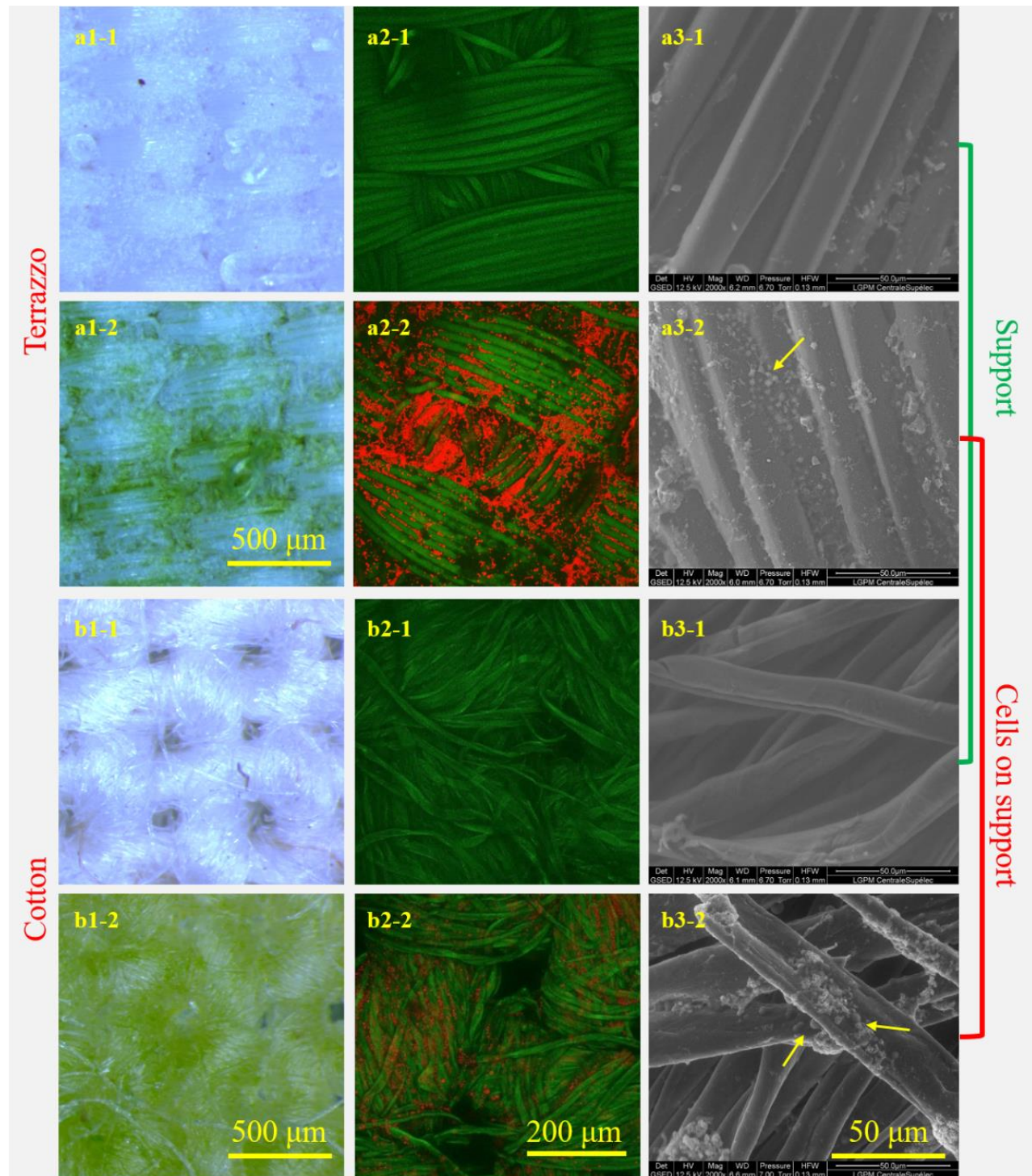
15

16 *3.2. Biofilm structure on Terrazzo and Cotton*

1 The micro-texture of Terrazzo and Cotton and biofilm structure on both textiles were
2 investigated using a stereomicroscope, a CLSM, a SEM (Fig. 3) and OCT (Fig.
3 S2_supplementary data). Terrazzo exhibited tightly-woven fibers with no clearly defined pores
4 (Fig. 3a) while Cotton fibers were loosely knitted resulting in higher porosity (Fig. 3b).

5 From Fig. 3, it appears that the cells did not cover uniformly the entire fabric at day 3. Cell
6 distribution patterns seemed different for the two supports. Indeed, cells mostly distributed on
7 and in between the tightly-woven fibers, forming cell clusters on the top surface of Terrazzo
8 while it seems that they did attach and grow mainly on the loosely connected fibers all through
9 Cotton's depth.

10



1

2 **Fig. 3** Microscopic structural observation of supports and cells (pre-acclimated to $50 \mu\text{mol}$

3 $\text{photons m}^{-2} \text{s}^{-1}$) attached on their fibers at day 3 (A, a-Terrazzo, b-Cotton. a1 and b1 represent

4 stereomicroscope images, a2 and b2 represent CLSM images, a3 and b3 show ESEM images.

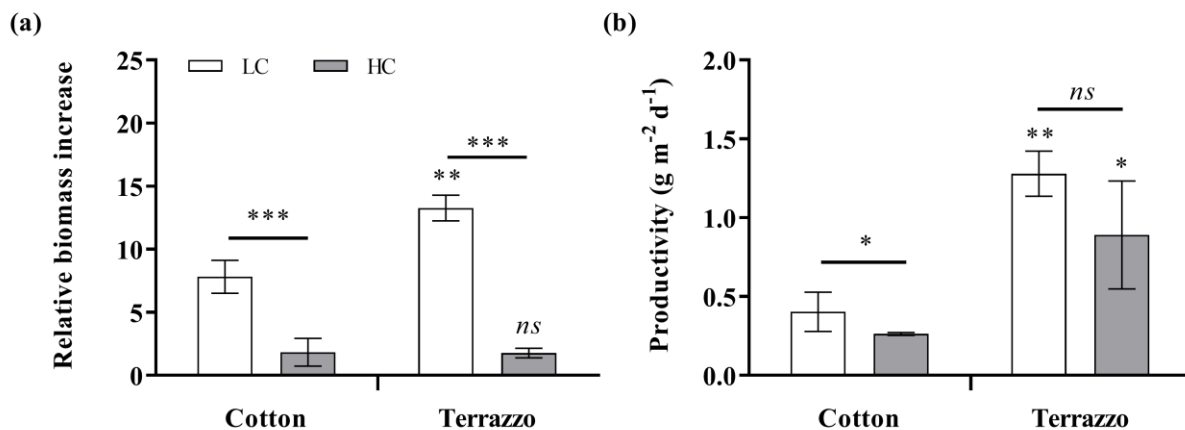
1 Red signal in CLSM images and yellow arrows in SEM images indicate cell or cells clusters on
2 the support fibers)

3

4 3.3. Support and inoculum density affect sessile cells growth, activity, composition and 5 biofilm productivity

6 Relative biomass increase (Rc) for Cotton and Terrazzo inoculated with $50 \mu\text{mol m}^{-2} \text{s}^{-1}$ pre-
7 acclimated cells is illustrated in Fig. 4a. Results show that, regardless of the support material, a
8 higher Rc (6-7 times) was obtained for the LC-inoculated biofilms than those inoculated with HC
9 ($P < 0.001$). On the other hand, productivity was ~ 3.2 times higher for Terrazzo compared to
10 those of Cotton (Fig. 4b, $P < 0.05$) regardless of the inoculum density, suggesting an impact of
11 the support on biofilm development.

12



13

14

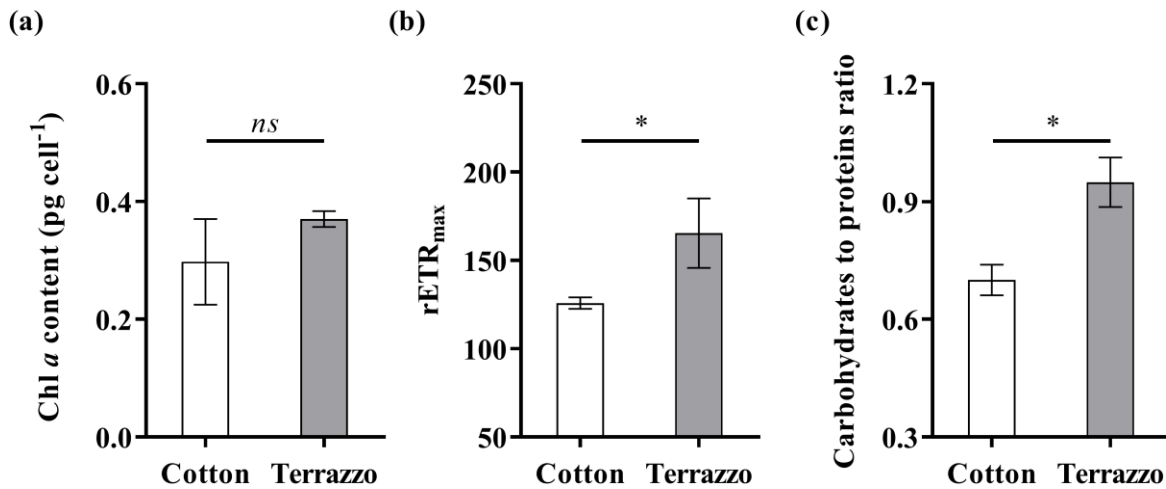
15 **Fig. 4** Effect of support and initial cell density (pre-acclimated to $50 \mu\text{mol photons m}^{-2} \text{s}^{-1}$) on
16 relative biomass increase (a) and biomass productivity (b) after 3-days cultivation of *C. vulgaris*
17 biofilms. All the results were shown as mean value \pm SD, $n = 3$; Bars with ***, ** and *

1 respectively depict the statistical differences between the immobilized cultures at $P < 0.001$, $P <$
2 0.01 and $P < 0.05$, and ns represents no difference

3

4 In order to get a deeper understanding on the effect of the support material on bioprocess
5 productivity, which is seldom studied, physiological properties of the cells grown on Terrazzo
6 and Cotton in LC condition (i.e., the cell density that improved biomass increase, Fig. 4a) were
7 characterized. Interestingly, differences in photosynthetic activity and composition of cells
8 developed on Terrazzo and Cotton were found (Fig. 5). Similar maximum quantum yield (F_v/F_m
9 around 0.7, Table S2_supplementary data) and cellular Chl *a* ($P > 0.05$, Fig. 5a) were measured
10 for cells on both supports but the cells on Terrazzo presented a higher electron transport capacity
11 (1.32 times) compared to those on Cotton (Fig. 5b, $P < 0.05$). In addition, no significant
12 difference in cell volume and photosynthetic activity parameters other than $rETR_{max}$ (alpha, E_k ;
13 Table S2_supplementary data and Fig. 5b) were measured while a higher relative pool of
14 carbohydrates (1.36-fold) was measured for sessile cells on Terrazzo (Fig. 5c, $P < 0.05$).

15



1
 2 **Fig. 5.** Chl *a* content (a), relative maximum electron transport rate (rETR_{max}, b) and
 3 carbohydrates to proteins ratio (c) of *C. vulgaris* biofilms (with the pre-acclimated inoculum at 50
 4 $\mu\text{mol m}^{-2} \text{s}^{-1}$) grown on Cotton and Terrazzo after 3-days cultivation at LC condition. All the
 5 results were shown as mean value \pm SD, $n = 3$; Bars with * represent the statistical differences
 6 between the immobilized cultures on two supports at a level of $P < 0.05$, and *ns* represents no
 7 difference

8

9 *3.4. Light-history of inoculum cells affects biofilm growth and productivity*

10 Table 1 displays the physiological properties of inoculum cells. HC-acclimated cells had
 11 higher growth rate (1.38 times, $P < 0.01$), smaller volume (0.69 times, $P < 0.01$), lower cellular
 12 Chl *a* quota (0.54 times, $P < 0.001$) and higher electrons transport capacity (rETR_{max}, 1.2 times, P
 13 < 0.01) when compared to their LC-acclimated counterparts. Both populations had no difference
 14 in cellular biochemical composition ($P > 0.05$).

15

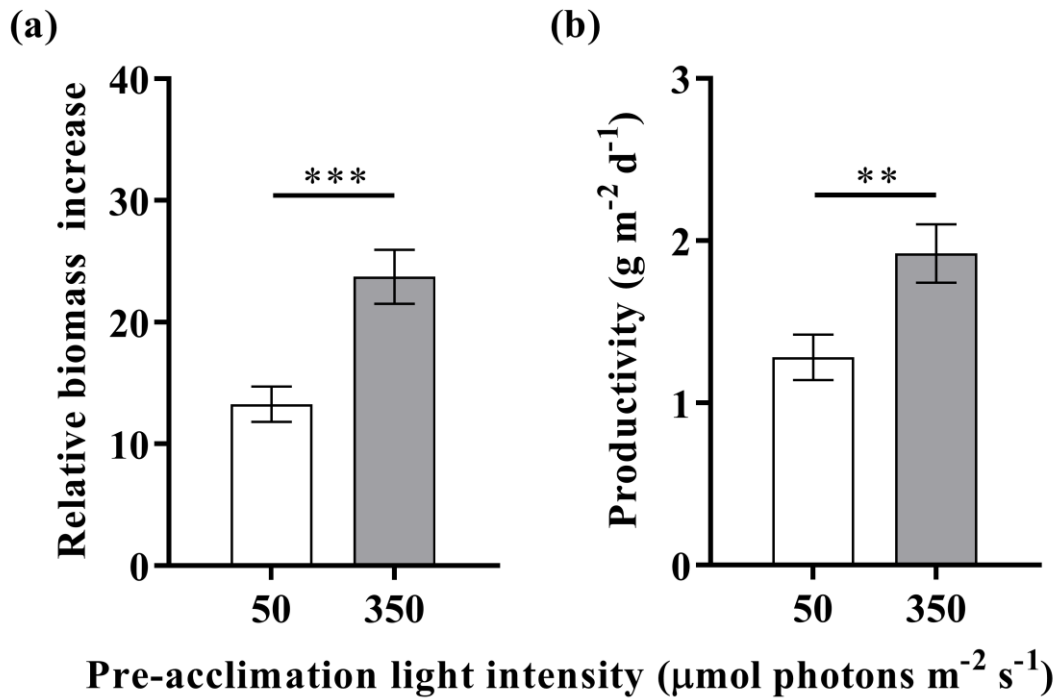
1 **Table 1** Physiological traits of inoculum cells pre-acclimated to low (LL, 50 $\mu\text{mol photons m}^{-2} \text{s}^{-1}$)
 2 1) and high light (HL, 350 $\mu\text{mol photons m}^{-2} \text{s}^{-1}$)

Cell traits	Pre-acclimation light intensity ($\mu\text{mol photons m}^{-2} \text{s}^{-1}$)		
	50 (LL)	350 (HL)	<i>P</i>
Growth rate (d^{-1})	1.09 \pm 0.20	1.50 \pm 0.25	0.0012
Cell volume (μm^3)	56.7 \pm 8.1	32.3 \pm 3.2	0.0043
Chl <i>a</i> (pg cell $^{-1}$)	0.46 \pm 0.04	0.26 \pm 0.04	0.0007
rETR _{max}	181.3 \pm 17.2	216.7 \pm 24.7	0.0051
F _v /F _m	0.73 \pm 0.02	0.60 \pm 0.05	< 0.0001
Carbohydrates to proteins ratio	0.79 \pm 0.03	0.79 \pm 0.06	0.8873
Lipids to proteins ratio	0.15 \pm 0.01	0.16 \pm 0.00	0.7273

3
 4 Since lower cell densities seemed to allow immobilized cells to attain higher productivities
 5 and faster growth, the effect of light-history of the inoculum was assessed only at low densities
 6 (LC).

7 Fig. 6a presents the relative biomass increase and productivity of biofilms developed on
 8 Terrazzo from inoculum cells photo-acclimated to low and high light intensities. An increase in
 9 R_c (1.8 times, *P* < 0.001, Fig. 6a) and an improvement in productivity (1.5 times, *P* < 0.01, Fig.
 10 6b) were observed for the HL biofilm (biofilm formed from cells photo-acclimated to High Light;
 11 350 $\mu\text{mol photons m}^{-2} \text{s}^{-1}$) compared to those exposed to low light intensity (LL biofilm, biofilm
 12 formed from cells photo-acclimated to Low Light; 50 $\mu\text{mol photons m}^{-2} \text{s}^{-1}$).

13



1
 2 **Fig. 6** Relative biomass increase (a) and biomass productivity (b) of 3-day *C. vulgaris* biofilms
 3 (inoculated with the pre-acclimated cells to 50 and 350 $\mu\text{mol photons m}^{-2} \text{s}^{-1}$) grown on Terrazzo
 4 at LC-conditions. All the results were shown as mean value \pm SD, $n = 3$; Bars with *** and **
 5 respectively depict the differences between immobilized cultures at $P < 0.001$ and $P < 0.01$

6
 7 **4. Discussion**

8 With the development of biofilm-based systems for microalgae cultivation, more information
 9 and understanding are required to operate them efficiently. Many studies have focused on long-
 10 term development (i.e., from weeks to months) of microalgae biofilms as a function of several
 11 operational factors such as light intensity, temperature, nutrients and shear stress (Schnurr et al.
 12 2014; Roostaei et al. 2018; Fanesi et al. 2019, 2021). However, only few tried to understand how
 13 the first operational steps (e.g. choice of substrate characteristics and light-history of the cells)

1 affect biofilm growth (Irving and Allen 2011; Genin et al. 2014). In this study, we followed a
2 precise experimental set-up to select promising initial conditions for biofilm development on
3 textile supports.

4 One of the first steps in biofilm development is represented by the adhesion of cells to a solid
5 substrate (Moreno Osorio et al. 2020). The choice of an optimal support is therefore of paramount
6 importance to promote cell attachment. We tested five fabrics with different characteristics, in
7 terms of chemical functional groups, texture and physical properties in order to target a promising
8 support for biofilm development (Table S1_supplementary data). In accordance with the
9 literature (Cui et al. 2013; Gross et al. 2016), the ability of the supports investigated in this work
10 to retain *C. vulgaris* was strongly dependent on their relative pore opening surface area, chemical
11 properties and the degree of hydrophobicity. The highest cell areal density and the lowest cell
12 detachment were obtained for the fabric “Terrazzo”, which is a polyamide-based textile (Fig. 2).
13 The dominant functional groups C=O in amide I and N-H bending in amide II (only detected on
14 this support) together with small mesh openings (Fig. 1, Fig. S1_supplementary data) seemed to
15 be responsible for the higher capacity of this support to retain *C. vulgaris* on its surface. This
16 fabric was therefore selected as a promising support for biofilm growth and compared to a cotton-
17 based fabric (Cotton, in our study) that is typically used in microalgae biofilm studies
18 (Christenson and Sims 2012; Gross et al. 2013; Moreno Osorio et al. 2020; In-na et al. 2022).

19 In aquatic ecosystems, substrates heterogeneity creates a variety of benthic environmental
20 niches that allows the maintenance of important population and community processes such as
21 primary production (Cardinale et al. 2002; Vivier et al. 2021). Similarly, fabrics with different
22 topographies and physico-chemical properties may create multiple niches that can stimulate
23 specific physiological responses of the immobilized microalgae. Indeed, when *C. vulgaris* was
24 immobilized on polyamide (Terrazzo) or cotton-based (Cotton) fabrics we found that not only the

1 nature of the substrate alters their productivity, but it also affects their physiological state in terms
2 of activity and macromolecular composition (Fig. 5). It is not surprising that on both fabrics
3 (polyamide and cotton-based) biomass increase was inhibited at high initial cell density, indeed a
4 decrease in light and/or nutrients availability in biofilms due to strong self-shading in densely
5 packed populations may occur as already reported in other works (Roberts et al. 2004; Huang et
6 al. 2016; Roostaei et al. 2018; Li et al. 2021). On the other hand, *C. vulgaris* presented 3.2 times
7 higher productivity on Terrazzo regardless of the initial cell density. This behavior may be related
8 to a different access to light for the immobilized cells on these two supports as a consequence of
9 fabrics micro-topography (Fig. 3, Table 1). Accordingly, cells grown on Terrazzo, mainly
10 distributed on the top of its surface, would have higher access to light than those embedded on
11 the porous and loosely-connected fibers in Cotton. Indeed, cell-shading and loosely connected
12 fibers in Cotton might reduce photons availability for photosynthesis for the cells distributed over
13 the support's depth. The higher light availability on the polyamide-based fabric may thus explain
14 the greater photosynthetic capacity ($rETR_{max}$) (Fig. 5b) and in turn the greater biomass increase,
15 higher productivity and carbohydrates pool observed for this fabric (Fig. 4 and Fig. 5c). Our data
16 is consistent with results of Vivier et al. (2021) who confirmed that support micro-topography
17 provided peculiar micro-habitats impacting biofilm biomass, photosynthetic capacity and
18 efficiency. Also, different cells-distribution patterns due to specific micro-textures of supports
19 have also been documented in previous works (Cui et al. 2013; Huang et al. 2018). Nevertheless,
20 experiments using techniques that can spatially resolve metabolic changes such as imaging PAM
21 and oxygen micro-profiling will be necessary to prove our hypothesis.

22 The final aim of this study was to test whether the light-history of microalgae could impact
23 early stages of biofilm formation. The inoculum of biofilm-based systems is often represented by
24 a planktonic microalgae population where cells are shifting from a planktonic to a benthic life

1 style (Moreno Osorio et al. 2020). Choosing cells that could best fit, from a physiological point of
2 view, the new cultivation conditions may shorten the lag-phase or even avoid the collapse of the
3 system. Corcoll et al. (2012) found for example that the light-history of phototrophic biofilms
4 was an essential factor in defining their response to Zn exposure. As expected, light intensity
5 affected the physiological traits of the inoculum with all the parameters indicating a classical
6 light acclimation strategy (Table 1). Interestingly, the light-history of the cells strongly affected
7 the rate of growth and the productivity once the cells were immobilized on the fabrics (Fig. 6). In
8 particular, a high light intensity during the planktonic phase boosted the growth of the cells on the
9 fabrics, which exhibited 1.5 times higher productivity (Fig. 6b). The planktonic cells grown under
10 high-light exhibited a smaller volume, lower Chl *a* content and a higher photosynthetic rate
11 ($rETR_{max}$, Table 1). This is in agreement with studies showing that smaller cells with a higher
12 metabolic rate lead to a greater biomass accumulation (Urabe and Kagami 2001; Key et al. 2010).
13 Our data is also in line with findings described in Martínez et al. (2018) who predicted that, the
14 lower the chlorophyll quota (Chl *a/C*), the higher the maximal productivity achieved in a
15 suspended culture. In our case, it is possible that in biofilms formed by planktonic cells with a
16 lower Chl *a* content light penetrates deeper through the cell layers, influencing positively growth.
17 Similarly, Wang et al. (2015) found that in thick biofilms microalgae cells tend to decrease the
18 amount of chlorophyll to allow more light to penetrate in the deepest layers.

19 Our data confirm that the inoculation step (i.e. support properties, inoculum density and its
20 physiological status) is of paramount importance in microalgae production when using biofilm-
21 based cultivation approaches. A selection of tightly-woven textiles, low inoculum density of cells
22 pre-acclimated to an appropriate high light could improve the productivity of a biofilm-based
23 system (Cui et al. 2013; Gross et al. 2016).

24

5. Conclusions

The effects of inoculum density/physiology and support nature on biofilm growth/productivity, activity, and composition were evaluated. Results show a decrease in biofilm growth when using high inoculum density, probably associated to a reduction in light/nutrients availability. Support micro-texture affects cells distribution, consequently impacting biofilm formation and activity. A higher $rETR_{max}$ and carbohydrate/protein ratio were exhibited by cells grown on a polyamide-based fabric (Terrazzo), suggesting a higher light availability to cells than those on Cotton. Our study also suggests that inoculum physiology, poorly considered in literature, affects biofilm productivity. Higher productivities were reported for biofilms inoculated with cells photo-acclimated to high light. Therefore, our data confirm that in the inoculation step, the support selection and inoculum density/physiology must be carefully considered in order to optimize biofilm-based systems productivity.

Reference:

- Bischo HW, Bold HC (1963) Phycological studies IV. Some soil algae from enchanted rock and related algal species. University of Texas Publication: Austin, TX, USA
- Brockhagen B (2021) Improved growth and harvesting of microalgae *Chlorella vulgaris* on textile fabrics as 2.5D substrates. AIMS Bioeng 8:16 - 24.
<https://doi.org/10.3934/bioeng.2021003>
- Cardinale BJ, Palmer MA, Swan CM, et al (2002) THE INFLUENCE OF SUBSTRATE HETEROGENEITY ON BIOFILM METABOLISM IN A STREAM ECOSYSTEM. Ecology 83:412 - 422. [https://doi.org/10.1890/0012-9658\(2002\)083\[0412:TIOSHO\]2.0.CO;2](https://doi.org/10.1890/0012-9658(2002)083[0412:TIOSHO]2.0.CO;2)
- Christenson LB, Sims RC (2012) Rotating algal biofilm reactor and spool harvester for wastewater treatment with biofuels by-products. Biotechnol Bioeng 109:1674 - 1684.
<https://doi.org/10.1002/bit.24451>
- Chung C, Lee M, Choe E (2004) Characterization of cotton fabric scouring by FT-IR ATR spectroscopy. Carbohydr Polym 58:417 - 420.

- 1 <https://doi.org/10.1016/j.carbpol.2004.08.005>
- 2 Corcoll N, Bonet B, Leira M, et al (2012) Light history influences the response of fluvial biofilms
3 to Zn exposure. *J Phycol* 48:1411 - 1423. [https://doi.org/10.1111/j.1529-](https://doi.org/10.1111/j.1529-8817.2012.01223.x)
4 [8817.2012.01223.x](https://doi.org/10.1111/j.1529-8817.2012.01223.x)
- 5 Cui Y, Yuan W, Cao J (2013) Effects of surface texturing on microalgal cell attachment to solid
6 carriers. *Int J Agric Biol Eng* 6:44 - 54
- 7 De Assis LR, Calijuri ML, Assemany PP, et al (2019) Evaluation of the performance of different
8 materials to support the attached growth of algal biomass. *Algal Res* 39:101440.
9 <https://doi.org/10.1016/j.algal.2019.101440>
- 10 Fanesi A, Lavayssière M, Breton C, et al (2021) Shear stress affects the architecture and cohesion
11 of *Chlorella vulgaris* biofilms. *Sci Rep* 11:1 - 11. [https://doi.org/10.1038/s41598-021-](https://doi.org/10.1038/s41598-021-83523-3)
12 [83523-3](https://doi.org/10.1038/s41598-021-83523-3)
- 13 Fanesi A, Martin T, Breton C, et al (2022) The architecture and metabolic traits of monospecific
14 photosynthetic biofilms studied in a custom flow - through system. *Biotechnol Bioeng*
15 119:2459 - 2470. <https://doi.org/10.1002/bit.28147>
- 16 Fanesi A, Paule A, Bernard O, et al (2019) The architecture of monospecific microalgae biofilms.
17 *Microorganisms* 7:352. <https://doi.org/10.3390/microorganisms7090352>
- 18 Genin SN, Stewart Aitchison J, Grant Allen D (2014) Design of algal film photobioreactors:
19 Material surface energy effects on algal film productivity, colonization and lipid content.
20 *Bioresour Technol* 155:136 - 143. <https://doi.org/10.1016/j.biortech.2013.12.060>
- 21 Gross M, Henry W, Michael C, Wen Z (2013) Development of a rotating algal biofilm growth
22 system for attached microalgae growth with in situ biomass harvest. *Bioresour Technol*
23 150:195 - 201. <https://doi.org/10.1016/j.biortech.2013.10.016>
- 24 Gross M, Jarboe D, Wen Z (2015) Biofilm-based algal cultivation systems. *Appl Microbiol*
25 *Biotechnol* 99:5781 - 5789. <https://doi.org/10.1007/s00253-015-6736-5>
- 26 Gross M, Wen Z (2014) Yearlong evaluation of performance and durability of a pilot-scale
27 Revolving Algal Biofilm (RAB) cultivation system. *Bioresour Technol* 171:50 - 58.
28 <https://doi.org/10.1016/j.biortech.2014.08.052>
- 29 Gross M, Zhao X, Mascarenhas V, Wen Z (2016) Effects of the surface physico-chemical
30 properties and the surface textures on the initial colonization and the attached growth in
31 algal biofilm. *Biotechnol Biofuels* 9:1 - 14. <https://doi.org/10.1186/s13068-016-0451-z>
- 32 Hart R, In-na P, Kapralov MV, et al (2021) Textile-based cyanobacteria biocomposites for
33 potential environmental remediation applications. *J Appl Phycol* 33:1525 - 1540.
34 <https://doi.org/10.1007/s10811-021-02410-6>

- 1 Hillebrand H, Durselen CD, Kirschtel D, et al (1999) Biovolume calculation for pelagic and
2 benthic microalgae. *J Phycol* 35:403 – 424. [https://doi.org/10.1046/j.1529-](https://doi.org/10.1046/j.1529-8817.1999.3520403.x)
3 [8817.1999.3520403.x](https://doi.org/10.1046/j.1529-8817.1999.3520403.x)
- 4 Hoghoghifard S, Mokhtari H, Dehghani S (2016) Improving the conductivity of polyaniline-
5 coated polyester textile by optimizing the synthesis conditions. *J Ind Text* 46:611 – 623.
6 <https://doi.org/10.1177/1528083715594981>
- 7 Huang Y, Xiong W, Liao Q, et al (2016) Comparison of *Chlorella vulgaris* biomass productivity
8 cultivated in biofilm and suspension from the aspect of light transmission and microalgae
9 affinity to carbon dioxide. *Bioresour Technol* 222:367 – 373.
10 <https://doi.org/10.1016/j.biortech.2016.09.099>
- 11 Huang Y, Zheng Y, Li J, et al (2018) Enhancing microalgae biofilm formation and growth by
12 fabricating microgrooves onto the substrate surface. *Bioresour Technol* 261:36 – 43.
13 <https://doi.org/10.1016/j.biortech.2018.03.139>
- 14 In-na P, Lee J, Caldwell G (2022) Living textile biocomposites deliver enhanced carbon dioxide
15 capture. *J Ind Text* 51:5683S-5707S. <https://doi.org/10.1177/15280837211025725>
- 16 Irving TE, Allen DG (2011) Species and material considerations in the formation and
17 development of microalgal biofilms. *Appl Microbiol Biotechnol* 92:283 – 294.
18 <https://doi.org/10.1007/s00253-011-3341-0>
- 19 Ji B, Zhang W, Zhang N, et al (2014) Biofilm cultivation of the oleaginous microalgae
20 *Pseudochlorococcum* sp. *Bioprocess Biosyst Eng* 37:1369 – 1375.
21 <https://doi.org/10.1007/s00449-013-1109-x>
- 22 Johnson MB, Wen Z (2010) Development of an attached microalgal growth system for biofuel
23 production. *Appl Microbiol Biotechnol* 85:525 – 534. [https://doi.org/10.1007/s00253-](https://doi.org/10.1007/s00253-009-2133-2)
24 [009-2133-2](https://doi.org/10.1007/s00253-009-2133-2)
- 25 Kang E, Kim M, Oh JS, et al (2012) Electrospun BMIMPF6/nylon 6,6 nanofiber chemiresistors
26 as organic vapour sensors. *Macromol Res* 20:372 – 378. [https://doi.org/10.1007/s13233-](https://doi.org/10.1007/s13233-012-0043-0)
27 [012-0043-0](https://doi.org/10.1007/s13233-012-0043-0)
- 28 Key T, McCarthy A, Campbell DA, et al (2010) Cell size trade-offs govern light exploitation
29 strategies in marine phytoplankton. *Environ Microbiol* 12:95 – 104.
30 <https://doi.org/10.1111/j.1462-2920.2009.02046.x>
- 31 Kostajnšek K, Zupin Ž, Hladnik A, Dimitrovski K (2021) Optical assessment of porosity
32 parameters in transparent woven fabrics. *Polymers* 13:408.
33 <https://doi.org/10.3390/polym13030408>
- 34 Li SF, Fanesi A, Martin T, Lopes F (2021) Biomass production and physiology of *Chlorella*
35 *vulgaris* during the early stages of immobilized state are affected by light intensity and
36 inoculum cell density. *Algal Res* 59:102453. <https://doi.org/10.1016/j.algal.2021.102453>

- 1 Li T, Strous M, Melkonian M (2017) Biofilm-based photobioreactors: their design and improving
2 productivity through efficient supply of dissolved inorganic carbon. FEMS Microbiol Lett
3 364:. <https://doi.org/10.1093/femsle/fnx218>
- 4 López-Sandoval DC, Rodríguez-Ramos T, Cermeño P, et al (2014) Photosynthesis and
5 respiration in marine phytoplankton: Relationship with cell size, taxonomic affiliation,
6 and growth phase. J Exp Mar Biol Ecol 457:151 – 159.
7 <https://doi.org/10.1016/j.jembe.2014.04.013>
- 8 MacIntyre HL, Kana TM, Anning T, Geider RJ (2002) Photoacclimation of photosynthesis
9 irradiance response curves and photosynthetic pigments in microalgae and cyanobacteria.
10 J Phycol 38:17 – 38. <https://doi.org/10.1046/j.1529-8817.2002.00094.x>
- 11 Martínez C, Bernard O, Mairet F (2018) Maximizing microalgae productivity in a light-limited
12 chemostat. IFAC-Pap 51:735 – 740. <https://doi.org/10.1016/j.ifacol.2018.04.001>
- 13 Moreno Osorio JH, De Natale A, Del Mondo A, et al (2020) Early colonization stages of fabric
14 carriers by two *Chlorella* strains. J Appl Phycol 32:3631 – 3644.
15 <https://doi.org/10.1007/s10811-020-02244-8>
- 16 Moreno Osorio JH, Pinto G, Pollio A, et al (2019) Start-up of a nutrient removal system using
17 *Scenedesmus vacuolatus* and *Chlorella vulgaris* biofilms. Bioresour Bioprocess 6:1 – 16.
18 <https://doi.org/10.1186/s40643-019-0259-3>
- 19 Ozkan A, Berberoglu H (2011) Adhesion of *Chlorella vulgaris* on hydrophilic and hydrophobic
20 surfaces. pp 169 – 178
- 21 Post AF, Dubinsky Z, Wyman K, Falkowski PG (1984) Kinetics of light-intensity adaptation in a
22 marine planktonic diatom. Mar Biol 83:231 – 238. <https://doi.org/10.1007/BF00397454>
- 23 Roberts S, Sabater S, Beardall J (2004) Benthic microalgal colonization in streams of different
24 riparian cover and light availability. J Phycol 40:1004 – 1012.
25 <https://doi.org/10.1111/j.1529-8817.2004.03333.x>
- 26 Roostaei J, Zhang Y, Gopalakrishnan K, Ochocki AJ (2018) Mixotrophic microalgae biofilm: a
27 novel algae cultivation strategy for improved productivity and cost-efficiency of biofuel
28 feedstock production. Sci Rep 8:1 – 10. <https://doi.org/10.1038/s41598-018-31016-1>
- 29 Schnurr PJ, Espie GS, Allen DG (2014) The effect of light direction and suspended cell
30 concentrations on algal biofilm growth rates. Appl Microbiol Biotechnol 98:8553 – 8562.
31 <https://doi.org/10.1007/s00253-014-5964-4>
- 32 Shahzadi L, Zeeshan R, Yar M, et al (2018) Biocompatibility through cell attachment and cell
33 proliferation studies of nylon 6/chitosan/ha electrospun mats. J Polym Environ 26:2030 –
34 2038. <https://doi.org/10.1007/s10924-017-1100-8>
- 35 Shen Y, Yang T, Zhu W, Zhao Y (2017) Wastewater treatment and biofuel production through

- 1 attached culture of *Chlorella vulgaris* in a porous substratum biofilm reactor. J Appl
2 Phycol 29:833 – 841. <https://doi.org/10.1007/s10811-016-0981-6>
- 3 Sukenik A, Bennett J, Mortain-Bertrand A, Falkowski PG (1990) Adaptation of the
4 photosynthetic apparatus to irradiance in *Dunaliella tertiolecta*: a kinetic study. Plant
5 Physiol 92:891 – 898
- 6 Tsavatopoulou VD, Manariotis ID (2020) The effect of surface properties on the formation of
7 *Scenedesmus rubescens* biofilm. Algal Res 52:102095.
8 <https://doi.org/10.1016/j.algal.2020.102095>
- 9 Urabe J, Kagami M (2001) Phytoplankton growth rate as a function of cell size: an experimental
10 test in Lake Biwa. Limnology 2:111 – 117. <https://doi.org/10.1007/s102010170006>
- 11 Van Oss CJ, Chaudhury MK, Good RJ (1988) Interfacial Lifshitz-van der Waals and polar
12 interactions in macroscopic systems. Chem Rev 88:927 – 941.
13 <https://doi.org/10.1021/cr00088a006>
- 14 Vivier B, Clauquin P, Lelong C, et al (2021) Influence of infrastructure material composition and
15 microtopography on marine biofilm growth and photobiology. Biofouling 37:740 – 756.
16 <https://doi.org/10.1080/08927014.2021.1959918>
- 17 Wagner M, Horn H (2017) Optical coherence tomography in biofilm research: A comprehensive
18 review. Biotechnol Bioeng 114:1386 – 1402. <https://doi.org/10.1002/bit.26283>
- 19 Wang J, Liu J, Liu T (2015) The difference in effective light penetration may explain the
20 superiority in photosynthetic efficiency of attached cultivation over the conventional open
21 pond for microalgae. Biotechnol Biofuels 8:1 – 12. [https://doi.org/10.1186/s13068-015-](https://doi.org/10.1186/s13068-015-0240-0)
22 [0240-0](https://doi.org/10.1186/s13068-015-0240-0)
- 23 Webb WL, Newton M, Starr D (1974) Carbon dioxide exchange of *Alnus rubra*. Oecologia
24 17:281 – 291. <https://doi.org/10.1007/BF00345747>
- 25 Wellburn AR (1994) The spectral determination of chlorophylls *a* and *b*, as well as total
26 carotenoids, using various solvents with spectrophotometers of different resolution. J
27 Plant Physiol 144:307 – 313. [https://doi.org/10.1016/S0176-1617\(11\)81192-2](https://doi.org/10.1016/S0176-1617(11)81192-2)
- 28 Zhang W, Wang J, Wang J, Liu T (2014) Attached cultivation of *Haematococcus pluvialis* for
29 astaxanthin production. Bioresour Technol 158:329–335.
30 <https://doi.org/10.1016/j.biortech.2014.02.044>
- 31